Int. J. Electrochem. Sci., 16 **(2021)** Article Number: 211114, doi: 10.20964/2021.11.18

International Journal of
ELECTROCHEMICAL
SCIENCE
www.electrochemsci.org

A Novel Joint Estimation Method of State of Charge and State of Health Based on the Strong Tracking-Dual Adaptive Extended Kalman Filter Algorithm for the Electric Vehicle Lithium-Ion Batteries

Ran Xiong[1], *Shunli Wang*[1,*], *Carlos Fernandez*[2], *Chunmei Yu*[1], *Yongcun Fan*[1], *Wen Cao*[1], *Cong Jiang*[1]

[1] School of Information Engineering, Southwest University of Science and Technology, Mianyang 621010, China;
[2] School of Pharmacy and Life Sciences, Robert Gordon University, Aberdeen AB10-7GJ, UK.
[*]E-mail: 497420789@qq.com

Received: 26 July 2021 / *Accepted:* 1 September 2021 / *Published:* 10 October 2021

In order to enhance the efficiency of electric vehicle lithium-ion batteries, accurate estimation of the battery state is essential. To solve the problems of system noise statistical uncertainty and battery model inaccuracy when using the extended Kalman filter (EKF) algorithm to estimate the battery state, a novel joint estimation algorithm of SOC and SOH based on the strong tracking-dual adaptive extended Kalman filter (ST-DAEKF) is proposed. Based on the extended Kalman filtering algorithm, the fading factor is introduced into it to enhance the tracking ability. Meanwhile, the adaptive filter which can statistics the characteristics of time-varying noise is used to adjust the noise parameters of the system. The BBDST condition and the DST condition at 25 °C are used for simulation and verification in MATLAB. The results of the algorithm simulation show that under the BBDST condition, the maximum SOC error and the average error of the proposed algorithm are 3.41% and 0.99%, respectively, with the corresponding convergence time of 15 seconds. And under the DST condition, the corresponding data is 1.56%, 1.29%, and 20 seconds, respectively. At the same time, compared with the extended Kalman algorithm, the SOH estimation results of this algorithm also have a better estimation effect and reference value. Under the BBDST condition, the maximum SOH error and average error under this algorithm are 0.12% and 0.06%, with the corresponding data of 0.66% and 0.23% under the DST condition. The above data proves the superiority of the joint estimation algorithm.

Keywords: electric vehicle; lithium-ion batteries; Thevenin; state of charge; state of health; strong tracking-dual adaptive extended Kalman filter

1. INTRODUCTION

With the large-scale promotion of electric vehicles (EVs), the demand for high-power batteries represented by lithium-ion batteries is rapidly increasing. EVs have many strengths compared with

gasoline vehicles, including low noise, environmental friendliness, and high efficiency [1]. As a result, nowadays, using EVs as an alternative to diesel- and petrol-powered cars is highly regarded [2]. In this context, a high-tech battery is a crucial element for EVs. There are various types of batteries used as the dominant power source in EVs. Among them, lithium-ion batteries are the most popular due to their specific characteristics [3]. The use status of a lithium-ion battery can almost determine its life [4]. However, if the safety of the lithium-ion battery is not guaranteed, its usable capacity and life will be greatly reduced, causing accidents in this case [5]. The performance of the battery and the battery management system (BMS) are closely related to the safety of the battery system [6]. It is very necessary to establish a BMS for a lithium-ion battery, which is important for monitoring battery states [7-9]. In the battery states of electric vehicles, SOC and SOH are the main factors related to the safety of BMS and the operating status of the vehicle [10, 11]. Hence, the accurate estimation of SOC and SOH is essential for the BMS. The main responsibility of SOC is to indicate the operation status of the battery and to protect the battery from over-charging and over-discharging by limiting the battery voltage range[12]. On the other hand, SOH is used to describe battery aging and health, which is defined by capacity loss or resistance increment[13].

So far, various methods have been introduced to estimate SOC and SOH. These methods are mainly divided into direct methods and indirect methods[14]. Direct measurement methods mainly include the Coulomb counting method, open-circuit voltage method, and electrochemical impedance spectroscopy method. When considering the direct method, a formula determined by the physical properties of the battery is used to estimate the SOC. A popular direct method is the Coulomb count estimation described in detail by Lashway et al.[15]. When the initial value of SOC can be obtained, the whole SOC value can be estimated by this method, but it has high requirements for the accuracy of the initial value of the SOC because it is an open-loop method. The functional relationship between OCV and SOC can be calculated by obtaining a fixed discharge rate, and then the known OCV is used to find the corresponding SOC value in the relationship curve. This method is named the OCV method [16]. However, this method must be placed for a long time to start the measurement, so it is not appropriate to estimate the SOC in actual operation. Electrochemical impedance spectroscopy (EIS) is another method to directly estimate SOC and SOH [17-19].

On the other hand, the indirect method does not use a specific equation but instead uses a battery model or system specification mapping. One of the indirect methods is a data-driven estimation. An accurate model is not be required in the data-driven estimation method, so some modeling steps can be omitted. Typical data-driven estimation methods include fuzzy logic (FL)[20], neural network (NN) [21-24], deep learning[25, 26] and support vector machine (SVM) [13, 27, 28]. However, data-driven estimation methods need to calculate much data and they are complex to train. Another indirect method is a model-based estimation. Common models are roughly classified into three categories: electrochemical model (EM), equivalent circuit model (ECM), and electrochemical impedance model (EIM)[29-32]. Among them, ECM is the most common model. Several adaptive filters, such as extended Kalman filter, unscented Kalman filter, particle filter, recursive least squares, H infinity, random forests (RF), and Gaussian process regression (GPR) can be combined with this type of model [33-39]. The battery SOH can be calculated by the measured internal resistance or the usable capacity. However, the online real-time measurement is very difficult, so the model-based estimation methods can be used here

to estimate internal resistance or rated capacity. Shyh-Chin Huang et al. proposed a SOC and SOH estimation method that considered the instantaneous discharging voltage and its voltage drop per unit time as the model parameters related to the SOC function [40]. Nikolao Wassiliadis et al. investigated a dual extended Kalman filter algorithm to estimate SOC and SOH jointly [41]. In [42], Miaomiao Zeng et al. proposed a SOC and SOH joint estimation method based on the fuzzy unscented Kalman algorithm. Reference document [43] analyzed a SOC and SOH estimation method based on the dual extended Kalman and multivariate autoregressive model. Mehdi Gholizadeh et al. utilized a systematic mixed adaptive observer and EKF approach to estimate SOC and SOH [44].

In this paper, a Thevenin ECM is used, which is combined with recursive least square to identify the corresponding parameters, respectively, and then the capacity definition method is selected to calculate SOH, and finally under the premise that full consideration is given to the reasons for the estimation error of SOC, a joint SOC and SOH estimation method is proposed, which is based on the ST-DAEKF algorithm. This algorithm uses two extended Kalman filters to estimate the SOC and capacity of a lithium-ion battery. Among them, the filter which is used to estimate SOC is combined with a strong tracking filter and an adaptive filter. First of all, the introduction of a strong tracking filter can effectively reduce the influence of observation noise under complex conditions. Secondly, the adaptive filter is used to predict and correct the observed noise in real-time. They can effectively improve the accuracy of battery SOC estimation. The results of the simulation show that the joint estimation algorithm is not related to the initial value of SOC, with the convergence time of 15 seconds under BBDST condition, and at the same time, the SOH estimation results are better and more practical than the extended Kalman filter algorithm.

The rest of this paper is organized as follows: Section 2 introduces the mathematical analysis, including equivalent modeling, parameter identification, iterative calculation algorithm, and iterative calculation process. Among them, the iterative calculation algorithm reviews the implementation method of extended Kalman filtering, puts forward the strong-tracking-dual adaptive extended Kalman filtering algorithm on the basis of extended Kalman filtering algorithm in full consideration, and uses the ST-DAEKF algorithm to estimate the SOC and the capacity. Section 3 analyzes the relevant experimental results and discusses the conclusion and finally, the summary of the full text is presented in Section 4.

2. MATHEMATICAL ANALYSIS

2.1. Equivalent modeling

In order to estimate the charge state of lithium-ion batteries conveniently and accurately, it is an important process to select a suitable ECM of lithium-ion batteries. The characterization form and accuracy of the internal dynamic characteristics will affect the estimation results of the charged state to a great extent. The battery is a highly complex nonlinear electrochemical energy storage device, so it is difficult to accurately describe the interaction and reaction in the control process. At present, the common battery models include EMs, neural network models, ECMs, and so on. The modeling and calculation of the EMs are very difficult, and the computing power of the system may not meet the theoretical requirements and is not suitable for engineering applications. The neural network model needs a large

number of experimental data to estimate the charge state of the battery, and it is easy to make a big error if it is not operated properly. The equivalent circuit model uses the circuit reaction to simulate the internal reaction of the battery. The Thevenin model is an equivalent circuit model with a simple structure, which can accurately show the internal changes of lithium-ion batteries and meet the needs of general engineering applications. The Thevenin model uses series resistors and an RC circuit to simulate the internal characteristics of the battery. Compared with the Rint model, the Thevenin model adds an RC loop to characterize the internal polarization response of the battery. The internal resistance and RC circuit in this model can be used to characterize the dynamic characteristics of the battery. The Thevenin model is one of the most commonly used ECMs. Therefore, the Thevenin model is selected based on the above judgment, which is shown in Figure 1.

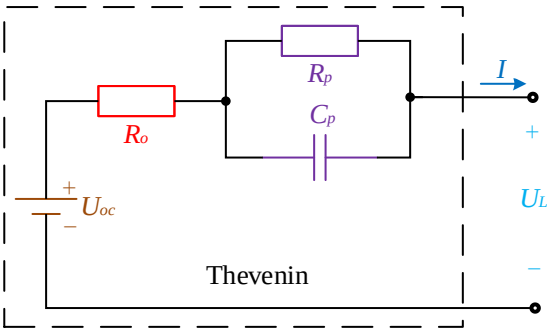

Figure 1. Thevenin equivalent circuit model

In Figure 1, R_o is the ohmic internal resistance, R_p is the polarization internal resistance, C_p is the polarization capacitance C_p, and U_L represents the battery terminal voltage. R_o can reflect the instantaneous change of battery voltage during charge and discharge. R_p and C_p can reflect the gradual change of battery voltage and the polarization effect inside the battery after charge and discharge. According to Kirchhoff's law, the equivalent circuit expression can be obtained from the Thevenin model:

$$\begin{cases} U_L = U_{oc} - U_o - U_p \\ I(t) = C_p \dfrac{dU_p}{dt} + \dfrac{U_p}{R_p} \end{cases} \tag{1}$$

In Figure 1, U_{oc}, R_o, R_p, C_p, and U_L are consistent with the physical meaning of the corresponding variables. U_p represents the voltage at both ends of R_p and C_p, and I represents the real-time current in the Thevenin equivalent circuit. Among them, the open-circuit voltage U_{oc} can be nonlinearly characterized by the SOC. The definitions of SOC and SOH can be written:

$$\begin{cases} SOC_t = SOC_{t_0} - \dfrac{\int_{t_0}^{t} \eta I(t)\eta dt}{C_0} \\ SOH_t = \dfrac{C_t}{C_0} \end{cases} \tag{2}$$

Among them, C_0 is the rated capacity of the battery, C_t is the capacity of the battery at time t, η is the Coulomb efficiency coefficient, I represents the charge and discharge current, and the direction of discharge is regarded as the positive direction. Besides, the capacity definition method is selected to calculate the SOH of battery. By using the knowledge of modern control theory, the equivalent model can be discretized. Combined with the SOC definition which is shown in Eq. (2), the state space variable $x_k = \left[SOC_k, U_{p,k} \right]^T$, the input variable $U_k = \left[I_k \right]$, and the output variable $y_k = \left[U_{o,k} \right]$ are selected. A discrete state space equation and observation equation can be obtained, as shown in the following formulas:

$$\begin{cases} \begin{bmatrix} SOC_{k+1} \\ U_{p,k+1} \end{bmatrix} = \begin{bmatrix} 1 & 0 \\ 0 & e^{-\frac{\Delta t}{\tau_p}} \end{bmatrix} \begin{bmatrix} SOC_k \\ U_{o,k+1} \end{bmatrix} + \begin{bmatrix} -\dfrac{\Delta t}{Q_N} \\ R_p \left(1 - e^{-\frac{T}{\tau_p}} \right) \end{bmatrix} I_k + \begin{bmatrix} w_{1,k} \\ w_{2,k} \end{bmatrix} \\ U_{o,k} = U_{oc,k} - R_{o,k} I_{k+} \begin{bmatrix} 0 \\ -1 \end{bmatrix}^T \begin{bmatrix} SOC_k \\ U_{p,k} \end{bmatrix} + v_k \end{cases} \tag{3}$$

Wherein, Δt is the sampling interval, $\tau_p = R_p C_p$. w is the state error, and v represents the measurement error, and their covariance matrices are Q and R, respectively.

2.2. RLS parameter identification

The methods for identification include offline and online algorithms. The offline algorithms have certain accuracy of identification, but they are only applied to some specific conditions. On the contrary, online algorithms can estimate the parameters with the change of working conditions and time. They have high estimation accuracy and great versatility. Therefore, using an online parameter identification method can better identify the model parameters, and the method used is the recursive least square (RLS) method[45]. It can reduce the error of the discharge rate change in the off-line parameter identification. According to the Thevenin model in Figure 1, the equation for the terminal voltage of the circuit can be obtained as shown in the following formula:

$$U_L(s) = U_{oc}(s) + I(s) \left(R_o + \frac{R_p}{1 + R_p C_p s} \right) \tag{4}$$

In Eq. (4), the equation can be obtained by Laplace transformation. Therefore, the following discrete system can be obtained through bilinear transformation:

$$y(k) = -ay(k-1) + bu(k) + cu(k-1) + v(k) \tag{5}$$

Wherein, a, b, and c are the parameters that require to be identified. To realize the least-squares principle for parameter identification, the discrete system equation can be expressed as the least-squares form in the following formulas:

$$\begin{cases} y(k) = x(k)^T \theta(k) + v(k) \\ x(k) = \left[y(k-1) \;\; u(k) \;\; u(k-1) \right]^T \\ \theta(k) = \left[-a \;\; b \;\; c \right]^T \end{cases} \tag{6}$$

Eq. (6)is the expression of least squares. The equations to calculate the unknown parameters of lithium-ion batteries are shown in the following formulas:

$$\begin{cases} \theta(k)=\theta(k-1)+K\cdot P(k-1)x(k)\left[y(k)-x(k)^{T}\theta(k-1)\right] \\ K=\left[x(k)^{T}P(k-1)x(k)+1\right]^{-1} \\ P(k)=\left[I-K\cdot P(k-1)x(k)x(k)^{T}\right]P(k-1) \end{cases} \tag{7}$$

After obtaining the parameter identification results, R_o, C_p, and R_p need to be calculated according to a, b, and c. The mathematical expression can be obtained as shown in the following formulas:

$$\begin{cases} G(s)=\dfrac{\dfrac{R_oT+R_pT+2R_pC_pR_o}{T+2R_pC_p}+\dfrac{R_oT+R_pT-2R_pC_pR_o}{T+2R_pC_p}z^{-1}}{1+\dfrac{T-2R_pC_p}{T+2R_pC_p}z^{-1}} \\ \dfrac{U_L(s)-U_{oc}(s)}{I(s)}=\dfrac{E(s)}{I(s)}=G(s), s=\dfrac{2\left(1-z^{-1}\right)}{T\left(1+z^{-1}\right)} \end{cases} \tag{8}$$

According to the principle of recursive least squares, the process of parameter calculation can be calculated as shown in the following formulas:

$$\begin{cases} a=\dfrac{T-2\tau}{T+2\tau} \\ b=\dfrac{R_oT+R_pT+2\tau R_o}{T+2\tau} \\ c=\dfrac{R_oT+R_pT-2\tau R_o}{T+2\tau} \end{cases} \tag{9}$$

The RLS method is a way to estimate the values of a, b, and c, and then according to Eq. (8)and Eq. (9), the ohmic resistance R_o, polarization capacitance C_p, and polarization resistance R_p can be calculated from the expression of the following formulas:

$$\begin{cases} R_o=\dfrac{b-c}{1-a} \\ \tau=R_pC_p=\dfrac{1-a}{2a+2} \\ R_p=(1+2\tau)b-2R_o\tau-R_o \\ C_p=\dfrac{\tau}{R_p} \end{cases} \tag{10}$$

Wherein, τ represents the time constant of the RC circuit. In other words, $\tau=R_pC_p$. T is the sampling interval. According to the above equations and the obtained parameters by the RLS method, R_o, C_p, and R_p of the Thevenin model can be estimated in real-time accurately.

2.3. Iterative calculation algorithm

The charging state of lithium-ion batteries is changed due to factors such as temperature, charging and discharging states, self-discharge and aging. Lithium-ion batteries have complex internal structures

and often exhibit strong nonlinear characteristics. These features make SOC estimation difficult. At present, the most commonly used methods for estimating battery SOC in the world include the ampere-hour integration method, open-circuit voltage method, neural network method, Kalman filter method, and corresponding methods of various extended forms. The charging and discharging process of lithium-ion batteries is a complex nonlinear process, and its SOC estimation accuracy is easily affected by the external environment under complex working conditions, making it difficult to quantify and analyze its mathematical model with conventional algorithms. In recent years, some new SOC and SOH estimation methods have been proposed. Among them, the extended Kalman filter algorithm, the unscented Kalman filter algorithm, and the adaptive Kalman filter algorithm are common algorithms used for state estimation. The core idea of the extended Kalman filter algorithm is to linearize the state equation of the nonlinear system. Then the Taylor formula is used to expand the nonlinear discrete function for linearization and the Kalman filter algorithm is adopted for processing. An algorithm which uses two extended Kalman filters to estimate the SOC and capacity of a lithium-ion battery is proposed in this paper. Among them, the filter which is used to estimate the SOC is combined with a strong tracking filter and an adaptive filter. First, the introduction of a strong tracking filter can enhance the tracking ability of the estimation results under complex conditions. Second, the adaptive filter is used to predict and correct the observed noise in real-time.

2.3.1. Kalman filtering calculation

Kalman Filter (KF) method is a filtering theory created by the state space theory in the time domain. It treats white noise as the observation noise of the system. The input/output equation is given in the time domain. The Kalman filter algorithm is mainly used to estimate linear time-invariant systems, using recursive linear minimum variance estimation method, using the observable output estimation error of the system to repair the unobservable state estimation error, thereby greatly reducing the noise in the data stream interference to reduce the error of estimation results. Kalman filter method first constructs a set of recursive equations that describe the characteristics of the battery system and can be recursively calculated to obtain a system state space expression containing signal and noise. SOC is one of the internal states, and then adopts a method based on the previous step. The estimated result and the current measurement data are processed by the mathematical method of optimized regression data, and the current optimal estimation result is obtained. The strength of this method is that the tracking ability is quite great and the dynamic SOC can be measured; however, the Kalman filter method requires high accuracy of the battery model, and the calculation is complicated.

The essence of the Kalman filter method is actually the ampere-hour integration method. While monitoring the external current, the collected voltage value is used to make certain corrections. When using the Kalman filter method to estimate SOC, an equivalent model needs to be established, and the accuracy of the Kalman algorithm is closely related to the accuracy of the model. The standard Kalman filter is only widely used in linear systems. The nonlinear system is first subjected to linearization preprocessing so that KF can be used. Its advantages and disadvantages are very obvious, and its advantage is a high accuracy, even in the case of severe current fluctuations and noise, it also has a good

correction effect. The disadvantage is that an accurate battery model needs to be established, and at the same time the algorithm requirements are higher.

The KF method is an effective method in the SOC estimation algorithm of lithium-ion batteries. It can continuously correct the current estimated value through the Kalman gain, quickly track the true value of the SOC in the continuous loop iterative operation process, and obtain the optimal estimated value in terms of the minimum mean square error. The algorithm has a fast speed of convergence and high accuracy of estimation. It can correct the initial error of the battery estimation and has a certain inhibitory effect on the interference noise.

When the KF method is adopted to estimate the battery SOC, the battery charging and discharging current is used as the input signal, the terminal voltage is used as the output signal, and the state of the system is continuously updated through the error between the observed value of the terminal voltage and the estimated value of the SOC, so as to obtain the minimum variance estimates the SOC value. Kalman filter is to obtain the dynamic estimation of the target by using the minimum mean square error criterion in the case of linear Gaussian. The basic flow chart of the KF algorithm is shown in Figure 2.

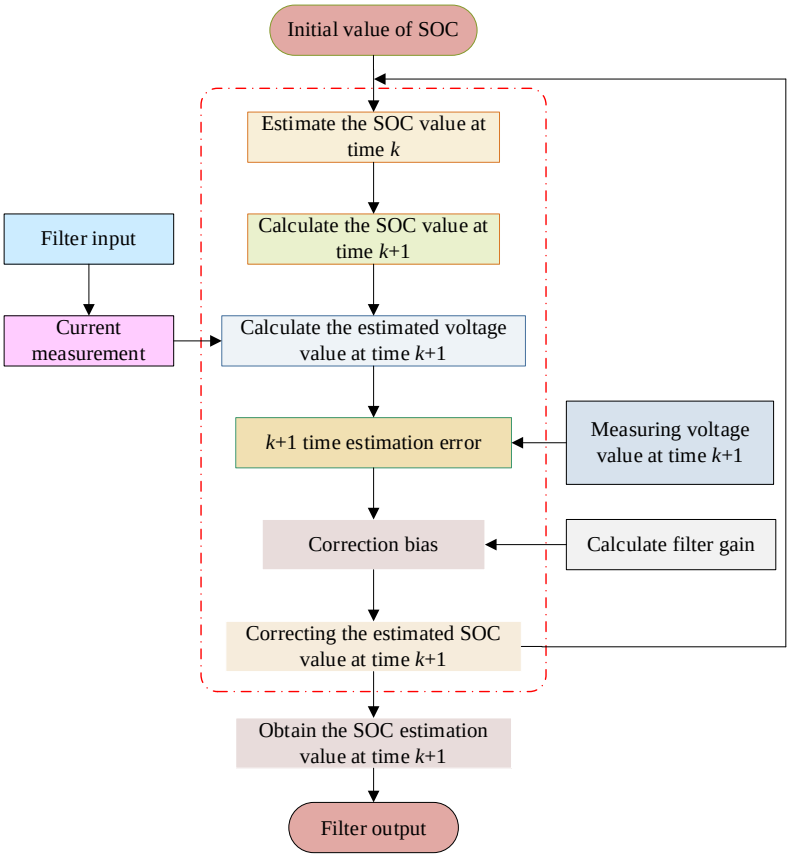

Figure 2. The KF algorithm flow chart

The basic idea of the Kalman Filter is to make the optimal estimation of the state of the power system with the smallest variance. It is an autoregressive data processing algorithm. The battery cell is

regarded as a power system, and the SOC is a state of the system. The algorithm estimates the estimated value of the current state variable based on the optimal value of the state variable at the previous moment and the difference between the actual value of the observed value and the estimated value, so the algorithm is recursive and its reliability is guaranteed. However, it is worth noting that the KF algorithm is only widely used in linear systems. In this algorithm, the state equation and observation equation after the linear system discretization are as follow:

$$\begin{cases} x_k = A_{k-1}x_{k-1} + B_{k-1}u_{k-1} + w_{k-1} \\ y_k = C_{k-1}x_k + D_k u_k + w_k \end{cases} \quad (11)$$

Wherein, x_k and x_{k-1} represent the system state variable at time k and k-1, respectively. u_k is the system input variable and y_k is the system observed value at time k. A_k is the transfer matrix of state x from k-1 to k, which predicts system variables. B_k is the system control input matrix and C_k is the system measurement matrix, which drives the observation and measurement of the forecast system. D_k is the feedforward matrix.

Kalman filtering is a filtering method in the time domain. A state-space model is adopted to describe the linear system. The process noise and observation noise of the system are not the objects to be filtered. Their statistical characteristics are the information that needs to be used in the estimation process. The calculation process is a process of continuous prediction and correction. There is no need to store large amounts of data during calculations. Once new data is observed, a new filter value can be calculated, which is very suitable for real-time processing and computer implementation. KF can only be used in linear systems, so certain linearization preprocessing is required when used in non-linear systems. The advantage of KF is that it has high accuracy and is suitable for environments with severe current fluctuations. Even in the presence of noise, it has a great effect of correction on the initial value. But its disadvantage is the need to establish an accurate model because when using the KF to estimate, it is necessary to constantly predict and update the space state equation of the model. At the present stage, the commonly used improved KF include extended Kalman filter (EKF), unscented Kalman Filter (UKF)[46], cubature Kalman filter (CKF)[1, 47], and so on. The EKF algorithm is improved to be suitable for non-linear systems. It linearizes the nonlinear state-space model and then implements it using the basic Kalman filter algorithm. The UKF makes up for the shortcomings of EKF in the processing of nonlinear systems. The UKF algorithm uses the idea of probability distribution to deal with nonlinear problems. UKF is an algorithm that changes the nonlinear function by calculating the statistical value of the nonlinear random variable. However, the above improvement methods based on Kalman filtering also introduce some defects.

2.3.2. Strong tracking-dual adaptive Extended Kalman filtering

The classic Kalman filter algorithm estimates in the time domain and does not perform mutual conversion between the time domain and the frequency domain. Therefore, its calculations are not complicated and it can be well estimated in real-time. It is often used in linear systems. In reality, most systems are non-linear stochastic systems, such as lithium-ion battery SOC systems. Therefore, the extended Kalman filter algorithm is adopted to solve such problems. The extended Kalman filter

algorithm estimates the nonlinear system by linearizing the nonlinear state-space model to achieve accurate state estimation. The extended Kalman algorithm is a mathematical method that combines probability theory. Its basic idea is to calculate the optimal value of estimation based on the minimum variance. Its principle is to combine the state-space model of signal and noise. The extended Kalman algorithm is a transformation based on the classic Kalman algorithm in non-linear systems. In this algorithm, the state transition function and the measurement function are subjected to the first-order Taylor expansion, and the influence of higher-order terms on the system is ignored, and the approximate linear space equation is obtained. Then, it is calculated according to the classical Kalman algorithm, which is widely adopted in discrete non-linear systems.

When using EKF to estimate the battery SOC, SOC is treated as a component in the state vector, and the current is used as the control variable in the input parameter, and the output is the terminal voltage calculated by the equivalent model. Both the system noise and the observation noise are Gaussian white noise, and its variance is expressed for Q and R. This method is usually based on the state of the system and the measurement equation. The predicted state equation includes the ampere-hour integration method for calculating the SOC, and the observation equation reflects the ECM of the lithium-ion battery. The accuracy of using the EKF algorithm to estimate the SOC largely depends on the accuracy of the equivalent model, so it is essential to establish an apposite equivalent model for lithium batteries. The expression equations and observation equations of the discrete non-linear system space as shown in the following formulas:

$$\begin{cases} X_{k+1} = f\left(X_k, k\right) + w_k \\ Z_k = h\left(X_k, k\right) + v_k \end{cases} \tag{12}$$

In Eq. (12), the first equation represents the state equation, and the second equation represents the observation equation. k is the discrete-time, X_k is the state value, Z_k is the observed value, w_k and v_k are the state error and the observation error respectively, that is, independent Gaussian white noise. When dealing with the non-linear problem of lithium-ion batteries, the first-order Taylor series expansion method can be used to expand its application in non-linear systems, that is, the first-order Taylor expansion of the non-linear functions f(*)and h(*), and the result is considered Is the best estimate at k time point. The expansion result is shown in the following formulas:

$$\begin{cases} f\left(X_k, k\right) \approx f\left(\hat{X}_k, k\right) + \left.\dfrac{\partial f\left(X_k, k\right)}{\partial X_k}\right|_{X_k = \hat{X}_k} \left(X_k - \hat{X}_k\right) \\ h\left(X_k, k\right) \approx h\left(\hat{X}_k, k\right) + \left.\dfrac{\partial h\left(X_k, k\right)}{\partial X_k}\right|_{X_k = \hat{X}_k} \left(X_k - \hat{X}_k\right) \end{cases} \tag{13}$$

After assigning values to A_k, B_k, C_k, and D_k, the values of A_k, B_k, C_k, and D_k can be obtained, as shown in the following formulas:

$$\begin{cases} A_k = \left.\dfrac{\partial f\left(X_k, k\right)}{\partial X_k}\right|_{X_k = \hat{X}_k}, B_k = f\left(\hat{X}_k, k\right) - A_k \hat{X}_k \\ C_k = \left.\dfrac{\partial h\left(X_k, k\right)}{\partial X_k}\right|_{X_k = \hat{X}_k}, D_k = h\left(\hat{X}_k, k\right) - C_k \hat{X}_k \end{cases} \tag{14}$$

After making a series of linear variations to A_k, B_k, C_k, and D_k, the nonlinear system is transformed into a linear system, and the transformed linear system is only related to state variables. Eq. (14) can be expressed linearly by the following formulas:

$$\begin{cases} X_{k+1} = A_k X_k + B_k + w_k \\ Z_k = C_k X_k + D_k + v_k \end{cases} \tag{15}$$

Eq. (15) contains a state space equation and an observation equation. Wherein, the meanings of A_k, B_k, C_k, and D_k are consistent with the correspondence in Eq. (11) The equation of the initial filtering state variable and its variance are as follow:

$$\begin{cases} X(0) = E[X(0)] \\ P(0) = Var[X(0)] \end{cases} \tag{16}$$

Using Eq. (15) to the discretization model and applying the Kalman algorithm to predict and estimate the state space equation, the recursive process of the extended Kalman algorithm can be obtained as shown in the following formulas:

$$\begin{cases} \hat{X}_{k+1}^{-} = f\left(\hat{X}_k\right) \\ \hat{P}_{k+1}^{-} = A_k \hat{P}_k A_k^T + Q_{k+1} \\ K_{k+1} = \hat{P}_{k+1}^{-} C_{k+1}^T \left(C_{k+1} \hat{P}_{k+1}^{-} C_{k+1}^T + R_{k+1}\right)^{-1} \\ \hat{X}_{k+1} = X_{k+1}^{-} + K_{k+1}\left[Z_{k+1} - h\left(X_{k+1}^{-}\right)\right] \\ \hat{P}_{k+1} = \left[I - K_{k+1} C_{k+1}\right] P_{k+1}^{-} \end{cases} \tag{17}$$

In Eq. (17), $\hat{X}_{k+1}^{-}$ is the prior state value directly calculated according to the state-space model and the previous time $\hat{X}_k$ at k+1, $\hat{P}_{k+1}^{-}$ is the corresponding prior covariance error matrix, and K_{k+1} is the corresponding Kalman gain. After the K_{k+1} at the current moment is used for correction, the optimal prediction estimates $\hat{X}_{k+1}$ and $\hat{P}_{k+1}$ of the current state value and the mean square error can be obtained, that is, the posterior state vector and the posterior covariance error. I is a unit matrix. Q and R are the variance matrices of w and v, respectively, and generally do not change over time.

The dual extended Kalman Filter (DEKF) algorithm is a method that adopts two Kalman filters to estimate the battery capacity and SOC respectively. One of the Kalman filters selects the EKF algorithm to estimate the SOC, which takes the SOC as the only state value and the battery capacity as a constant value. Another Kalman filter adopts the EKF algorithm to estimate the battery capacity. It takes the SOC as an input value and the battery capacity as a state value. The change in battery SOH can be obtained by predicting the attenuation change of the capacity. The schematic diagram of the DEKF algorithm is shown in Figure 3.

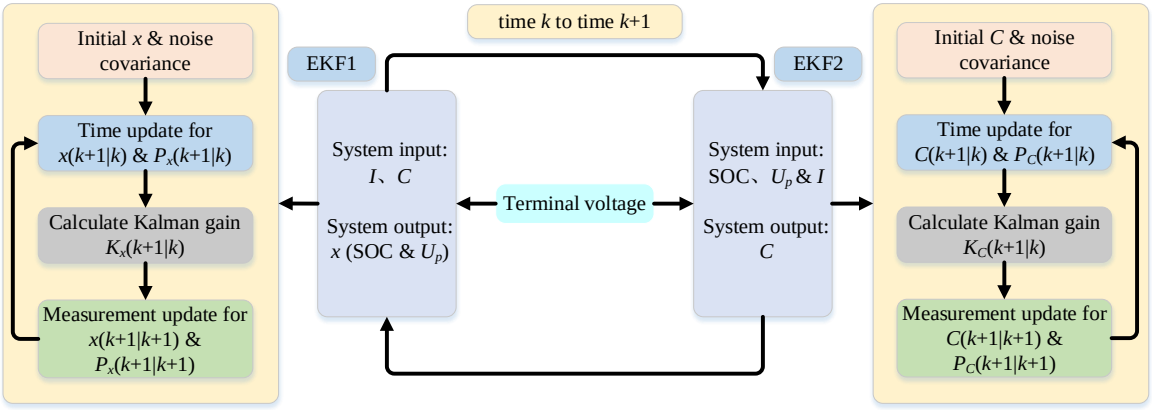

Figure 3. The schematic diagram of the DEKF algorithm

In Figure 3, capacity is represented by *C*. The DEKF algorithm can jointly estimate the SOC and SOH. In the joint process, the observed value can update and calculate the parameters to improve the accuracy of estimation. However, Eq. (17) is only one of the recursive processes of the dual extended Kalman filter in the ST-DAEKF algorithm. For another extended Kalman filter, it combines a strong tracking filter and an adaptive filter. For achieving the strong tracking characteristics of the filter, a couple of conditions need to be met during recursion, as shown in the following formulas:

$$\begin{cases} E\left(X_k - \hat{X}_k\right)\left(X_k - \hat{X}_k\right)^T = \min \\ E\left(\gamma_k \gamma_{k+j}^T\right) = 0 \quad k = 1,2,3,\cdots; \quad j = 1,2,3,\cdots \\ \gamma = Z_{k+1} - h\left(X_{k+1}^-\right) \end{cases} \tag{18}$$

To make the system have the ability to track sudden changes, a fading factor λ_k is introduced into the error covariance matrix of the EKF to strengthen the proportion of the current observation data. Besides, if the noise characteristics are always assumed to be Gaussian white noise, the actual estimated error value of the system state will be very different from the theoretically calculated error value. Therefore, the introduction of an adaptive filter can continuously estimate and modify the statistical characteristics of noise through the measurement data to reduce the error of estimation. The error covariance matrix after optimization is shown in the following formula:

$$\hat{P}_{k+1}^- = \lambda_{k+1} A_k \hat{P}_k A_k^T + \Gamma Q_{k+1} \Gamma^T \tag{19}$$

In Eq. (19), λ_{k+1} represents the fading factor and Γ is the noise drive matrix. When using the orthogonal principle given by Eq. (18) to solve the fading factor, the gradient method is needed. This method uses nonlinear programming to solve the optimal decay factor, and the amount of calculation is too large to realize online calculation. Therefore, this paper adopts the calculation method of sub-optimal fading factor, as shown in the following formulas[48]:

$$\lambda_k = \begin{cases} 1 & \left(e_k \le 1\right) \\ e_k = \dfrac{tr\left(N_k\right)}{tr\left(M_k\right)} & \left(e_k > 1\right) \end{cases} \tag{20}$$

Wherein, N_k and M_k can be expressed in the following formulas:

$$\begin{cases} N_k = V_k - \beta R_k - C_k \Gamma Q_{k-1} \Gamma^T C_k^T \\ V_k = \begin{cases} \gamma_1 \gamma_1^T & (k=1) \\ \dfrac{\rho V_{k-1} + \gamma_k \gamma_k^T}{1+\rho} & (k>1) \end{cases} \\ M_k = C_k A_{k-1} P_{k-1} A_{k-1}^T C_k^T \end{cases} \tag{21}$$

V_k is the residual covariance matrix; ρ is the forgetting factor with $0<\rho\leq 1$ and β is the weakening factor with $\beta\geq 1$. In this paper, the adaptive filter is a statistically large posterior sub-optimal unbiased estimator of noise based on measured values. The recursive process of input process noise Q and observation noise R is as follows:

$$\begin{cases} \hat{Q}_{k+1} = \dfrac{1}{k+1} G \sum_{i=0}^{k} \left(K_{k+1} \tilde{\gamma}_{k+1} \tilde{\gamma}_{k+1}^T K_{k+1}^T + P_{k+1} - A P_{k|+1k} A^T \right) G^T \\ G = \left(\Gamma^T \Gamma \right) \Gamma^T \\ \hat{R}_{k+1} = \dfrac{1}{k+1} \sum_{i=0}^{k} \left(\tilde{\gamma}_{k+1} \tilde{\gamma}_{k+1}^T - C P_{k|+1k} A^T C^T \right) \end{cases} \tag{22}$$

The adaptive filter can estimate Q and R online in real-time, and achieve the goal of continuous correction of the SOC estimation value, thereby realizing the adaptive correction function to achieve the effect of improving the accuracy of the SOC estimation. Therefore, the recursive process of the second improved Kalman filter combined with a strong tracking filter and an adaptive filter is shown in the following formulas[49]:

$$\begin{cases} \hat{X}_{k+1}^- = f\left(\hat{X}_k \right) \\ \hat{P}_{k+1}^- = \lambda_{k+1} A_k \hat{P}_k A_k^T + \Gamma Q_{k+1} \Gamma^T \\ K_{k+1} = \hat{P}_{k+1}^- C_{k+1}^T \left(C_{k+1} \hat{P}_{k+1}^- C_{k+1}^T + R_{k+1} \right)^{-1} \\ \hat{X}_{k+1} = X_{k+1}^- + K_{k+1} \left[Z_{k+1} - h\left(X_{k+1}^- \right) \right] \\ \hat{P}_{k+1} = \left[I - K_{k+1} C_{k+1} \right] P_{k+1}^- \end{cases} \tag{23}$$

In Eq. (23), the fading factor λ_{k+1} is introduced into the EKF algorithm to enhance the tracking ability. Meanwhile, the adaptive filter which can statistics the characteristics of time-varying noise is used to adjust the noise parameters of the system. It is worth noting that X, P, K, A, and C here are different from those in Eq. (17).

2.4. Iterate calculation process

In the Thevenin model, according to the relationship between voltage, current, and the ampere-hour integral principle, the state space equation can be obtained as shown in the following formulas:

$$\begin{cases} E(t) = U_L(t) + R_0 I(t) + u(t) \\ I(t) = \dfrac{u(t)}{R_p} + C_p \dfrac{du}{dt} \\ SOC(t) = SOC(t_0) - \dfrac{1}{C_0}\int_{t_0}^{t} \eta i(t)\, dt \end{cases} \tag{24}$$

In Eq. (24), E is the ideal voltage source, I is the current through the internal resistance R_o, C_0 is the rated capacity, η is the Coulomb efficiency coefficient and i represents the charge and discharge current. The direction of discharging is specified as the positive direction. The ST-DAEKF algorithm is adopted to estimate the SOC and battery capacity. The state equation and the observation equation of battery SOC are shown in the following formulas:

$$\begin{cases} x(k \mid k-1) = A^x_{k-1} x(k-1) + B^x_{k-1} i_{k-1} + w_k \\ y_k = h(x_{k-1}, i_{k-1}) + v_k = U_{oc} - R_p i_k - u_k + v_k \end{cases} \tag{25}$$

After linearizing the Eq. (25) by first-order Taylor expansion, the corresponding values of A_k^x, B_k^x, and C_k^x, of the Thevenin ECM in the Eq. (14) can be obtained as shown in the following formulas: A_k^x is the state transition matrix, B_k^x is the control matrix, and C_k^x is the observation matrix. The EKF algorithm is selected to estimate the target state, and there is no need to calculate the nominal trajectory in advance. The goal of solving the nonlinear equation is to make the noise zero. The extended Kalman algorithm is a linear approximate nonlinear process, so it can only be used with filtering errors.

$$\begin{cases} A^x_k = \begin{pmatrix} 1 & 0 \\ 0 & e^{-t/\tau} \end{pmatrix} \\ B^x_k = \begin{pmatrix} -\dfrac{t}{C_0} \\ R_p\left(1 - e^{-t/\tau}\right) \end{pmatrix} \\ C^x_k = \left(\dfrac{\partial u_{oc}}{\partial soc} \quad -1 \right)\Big|_{x_k = \hat{x}_k} \end{cases} \tag{1}$$

In order to estimate the current actual capacity of the battery, it is necessary to establish the system state equation about the capacity. Considering that there is no direct relationship between the capacity and the terminal voltage, it is necessary to construct a new observation equation. The discrete form of the SOC equation of state can be expressed by using the ampere-hour integration method of Eq. (24) as the moving term, which can be used as the observation equation for battery SOH estimation. The corresponding state equation and observation equation of battery capacity are shown in the following formulas:

$$\begin{cases} C(k+1) = C(k) + r(k) \\ z(k) = SOC(k) - SOC(k-1) + \dfrac{i(k)\Delta t}{C(k-1)} + e(k) \end{cases} \tag{27}$$

Since the capacity of the battery will decay as the number of battery cycles increases, an external noise $r(k)$ is introduced into the state equation for estimating the capacity to simulate the decay process of the battery capacity. The noise $r(k)$ is selected according to the change curve of capacity decay in the battery cycle charge and discharge test. $z(k)$ is the observation parameter, $e(k)$ represents a Gaussian

white noise with a mean value of 0. When $z(k)$ is zero, $A_k{}^C$ and $C_k{}^C$ can be obtained by applying extended Kalman according to Eq. (27), as shown in the following formulas:

$$\begin{cases} A_k^C = 1 \\ C_k^C = -\dfrac{\eta i \Delta t}{C^2} \end{cases} \tag{28}$$

Wherein, $A_k{}^C$ and $C_k{}^C$ are the state equation coefficient matrix and the observation equation coefficient matrix for estimating the battery capacity. According to Eq. (22) and EKF algorithm, the recursive process of input process noise Q and observation noise R is shown in the following formulas[50]:

$$\begin{cases} \hat{Q}_{k+1} = (1-d_k)\hat{Q}_k + d_k G\left(K_k \tilde{y}_{k+1} \tilde{y}_{k+1}^T K_k^T + P_{k+1} - A P_{k|+1k} A^T\right) G^T \\ \hat{R}_{k+1} = (1-d_k)\hat{R}_k + d_k \tilde{y}_{k+1} \tilde{y}_{k+1}^T - C P_{k|+1k} A^T C^T \end{cases} \tag{29}$$

The recursive process of the ST-DAEKF algorithm concludes with 4 steps. The first step is the initialization of the ST-DAEKF algorithm, as shown in the following formulas:

$$\begin{cases} \hat{C}_0 = E[C_0] \\ P_0^C = E\left[(C_0 - \hat{C}_0)(C_0 - \hat{C}_0)^T\right] \\ \hat{x}_0 = E[x_0] \\ P_0^x = E\left[(x_0 - \hat{x}_0)(x_0 - \hat{x}_0)^T\right] \end{cases} \tag{30}$$

In the second step, the covariance is predicted. When the EKF algorithm is adopted to estimate the battery capacity and SOC, the state prediction equations and the covariance prediction equations are shown in the following formulas:

$$\begin{cases} C(k+1|k) = C(k|k) \\ P_C(k+1|k) = P_C(k|k) + Q_C(k) \\ x(k+1|k) = A_x(k)x(k|k) + B_x(k)i(k) \\ P_x(k+1|k) = \lambda(k+1) A_x(k) \hat{P}_x(k|k) A_x^T(k) + \Gamma Q_x(k) \Gamma^T \end{cases} \tag{31}$$

The third step is to calculate the Kalman gain of SOC and then the state equation and the covariance equation of battery SOC are updated. The corresponding equations are as follows:

$$\begin{cases} K_x(k+1) = P_x(k+1|k) C_x^T(k+1)\left[C_x(k+1) P_x(k+1|k) C_x^T(k+1) + R_x\right] \\ \hat{x}(k+1|k+1) = x(k+1|k) + K_x(k+1)\left[y(k+1) - \hat{h}(k+1|k)\right] \\ P_x(k+1) = \left[I - K_x(k+1) C_x(k+1)\right] P_x(k+1|k) \\ SOC(k) = [1,0]\hat{x}(k) \end{cases} \tag{32}$$

The fourth step is calculating the Kalman gain of battery capacity and updating the state equation and covariance equation of capacity. The corresponding equations are shown in the following formulas:

$$\begin{cases} K_C(k+1) = P_C(k+1|k) C_C^T(k+1)\left[C_C(k+1) P_C(k+1|k) C_C^T(k+1) + R_C\right] \\ \hat{C}(k+1|k+1) = C(k+1|k) + K_C(k+1)\left[y(k+1) - \hat{h}(k+1|k)\right] \\ P_C(k+1) = \left[I - K_C(k+1) C_C(k+1)\right] P_C(k+1|k) \\ C(k) = \hat{C}(k) \end{cases} \tag{33}$$

To obtain the estimated SOC value and capacity value, it is necessary to loop Eq. (31)to Eq. (33) until the end of the ST-DAEKF algorithm. The two EKFs in the ST-DAEKF algorithm estimate the SOC and capacity at the same time to exchange information, as shown in Figure 4.

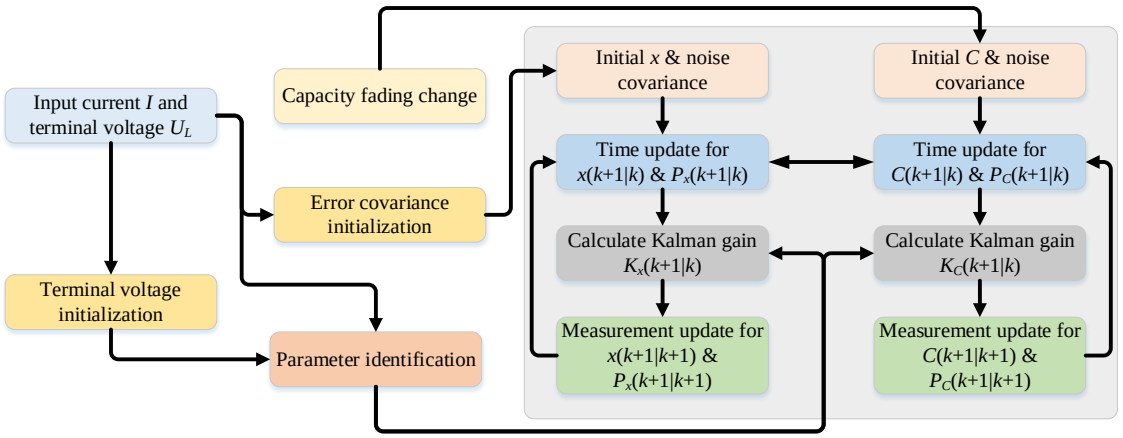

Figure 4. The flowchart of the ST-DAEKF algorithm

In Figure 4, the first extended Kalman filter estimates x which represents a fast-varying state, and the second extend Kalman filter simultaneously estimates C which represents a slow-varying parameter. Two extended Kalman filters transmit information to each other at each sampling point. The first EKF runs first to estimate the SOC value, and the voltage error is used to update the capacity value in the second EKF.

3. EXPERIMENTAL ANALYSIS

3.1. Test platform construction

During this experiment, all experimental process is performed in the power battery large-rate charge and discharge tester (BTS750-200-100-4) and the thermostat with a three-layer temperature control chamber (DGBELL-BTKS). Besides, the experimental equipment is connected to a high-configuration host computer that stores and calculates experimental data. The thermostat can effectively prevent measurement errors caused by temperature changes. The experimental test platform is shown in Figure 5.

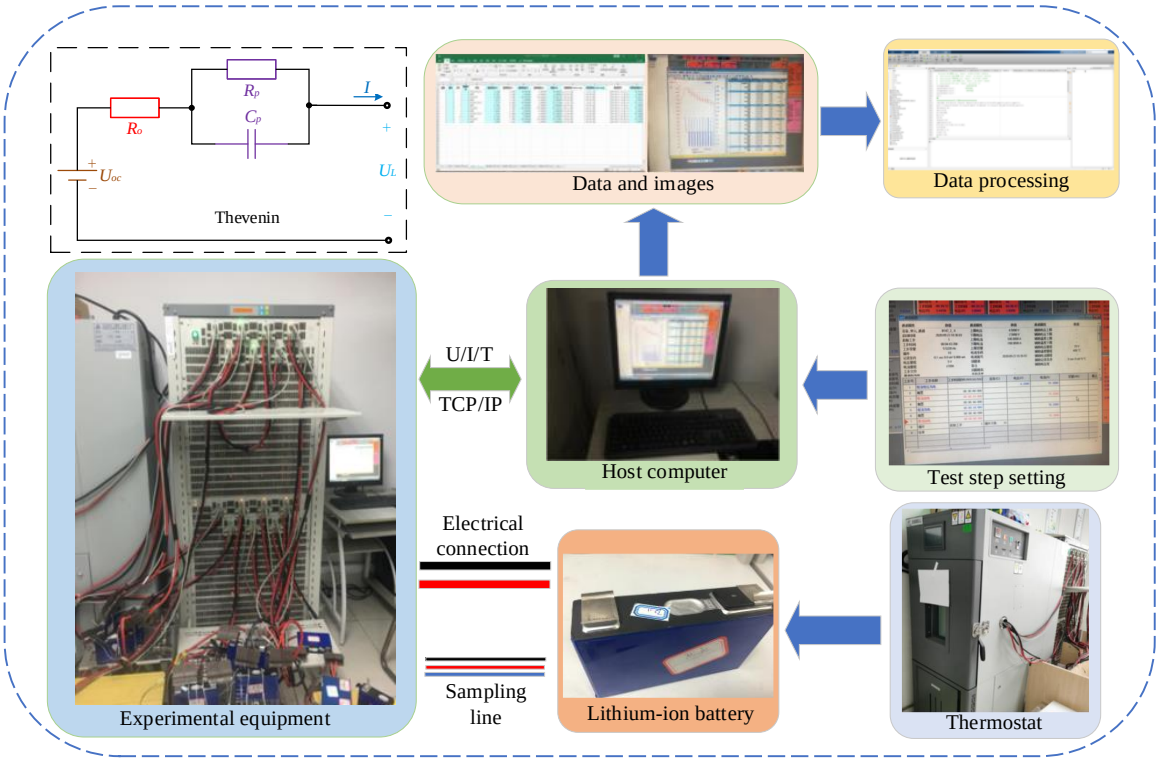

Figure 5. Experimental test platform

In this paper, a lithium-ion battery with a rated capacity of 70 Ah is selected for the experiment and the experimental temperature of the thermostat is set to be constant at 25 °C. Based on the above experimental test platform and its corresponding settings, the input values of the RLS method and the ST-DAEKF algorithm can be obtained to verify the reliability of the algorithm.

3.2. Identification experiments

Due to the difference in the dynamic characteristics of lithium-ion batteries during operation, the Beijing bus dynamic stress test (BBDST) condition and the dynamic stress test (DST) condition of a lithium-ion battery are carried out for online parameter identification. This section takes the BBDST working condition as an example to show the process of RLS online identification. The BBDST condition is obtained by collecting the real data of the Beijing bus, which collects the data of each link such as starting, acceleration, sliding, and so on. The specific steps for setting BBDST conditions are shown in Table 1.

Table 1. The steps of BBDST working condition

P_h（kW）	P_c（W）	Single step（s）	Grand total（s）	Working condition	P_h（kW）	P_c（W）	Single step（s）	Grand total（s）	Working condition
37.5	69	21	21	Start	4.5	9	16	150	Sliding
72.5	135	12	33	Accelerate	-15	-27	6	156	Brake
4.5	9	16	49	Sliding	72.5	135	9	165	Accelerate
-15	-27	6	55	Brake	92.5	174	6	171	Rapid acceleration
37.5	69	21	76	Accelerate	37.5	69	21	192	Accelerate
4.5	9	16	92	Sliding	4.5	9	16	208	Sliding
-15	-27	6	98	Brake	-35	-66	9	217	Brake
72.5	135	9	107	Accelerate	-15	-27	6	229	Brake
92.5	174	6	113	Rapid acceleration	4.5	9	71	300	Parking
37.5	69	21	134	Accelerate					

In Table 1, P_h is the real battery output power of the Beijing bus under starting, acceleration, sliding, braking, rapid acceleration, and parking conditions. Since the experimental object studied in this article is a lithium-ion battery cell, according to the various parameters of the battery, the power of each step is reduced in proportion to perform the BBDST condition and P_c is the output power after proportional reduction.

After importing the recorded data into the RLS method, the ohmic internal resistance R_o, the polarization internal resistance R_p, the polarization capacitance C_p and the open-circuit voltage U_{oc} can be identified online. The identification results are shown in Figure 6.

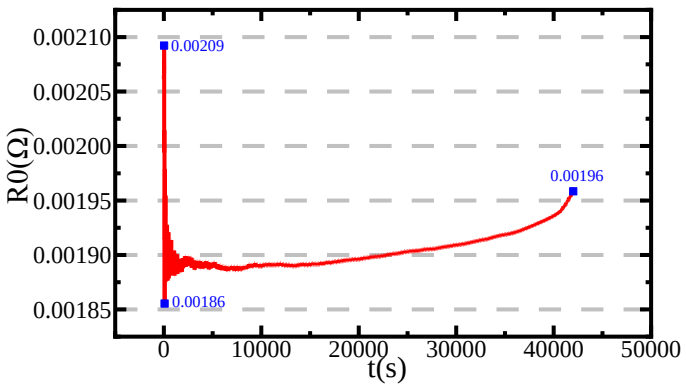

(a) Identification result of R_o

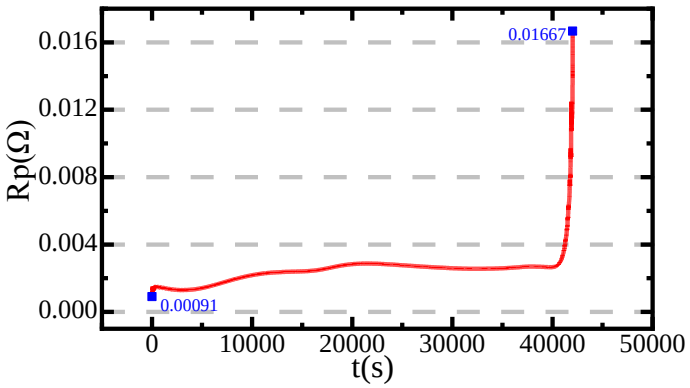

(b) Identification result of R_p

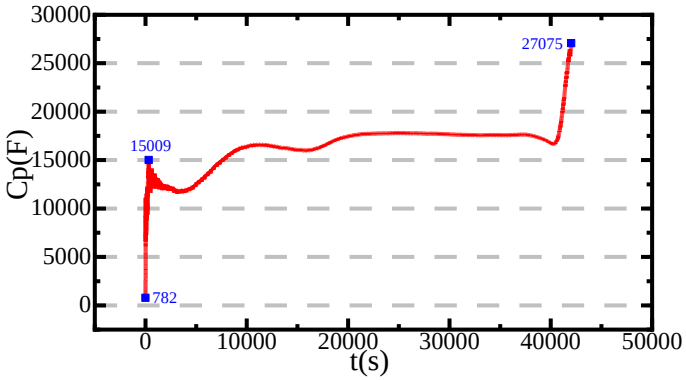

(c) Identification result of C_p

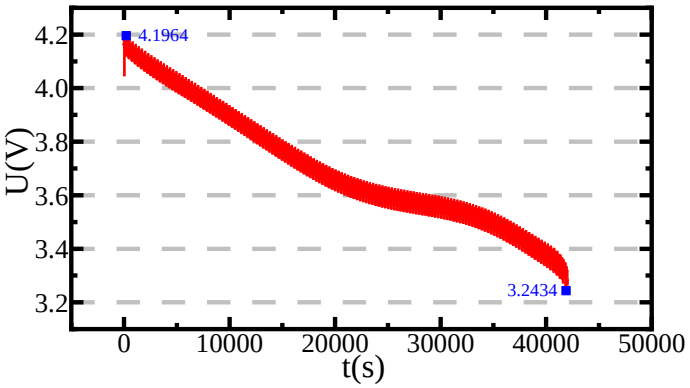

(d) Identification result of U_{oc}

Figure 6. Identification results of R_o, R_p, C_p, and U_{oc}

It can be seen from Figure 6(a) that as the decrease of SOC, the ohmic internal resistance R_o first fluctuates greatly in the early period, and then increases with a small change range and a slow change rate. Additionally, Figure 6(b) shows that the internal polarization resistance R_p tends to stabilize at first and increases suddenly in the end. And for C_p which is shown in Figure 6(c), it increases greatly in the early period, then gradually stabilizes, and finally increases rapidly. The fluctuation of the parameters is mainly caused by the charge and discharge rate. In Figure 6(d), the simulated U_{oc} can be found that trend is consistent with the actual BBDST working condition.

3.3. Complex condition analysis

To verify the convergence and traceability of the SOC estimation method based on the ST-DAEKF algorithm, the battery testing equipment (BTS750-200-100-04) provided by Shenzhen Yakeyuan Technology Co., Ltd. is used to conduct the BBDST working condition and the DST working condition on an AVIC ternary lithium-ion battery cell. The charts of experimental data under these two working conditions are shown in Figure 7.

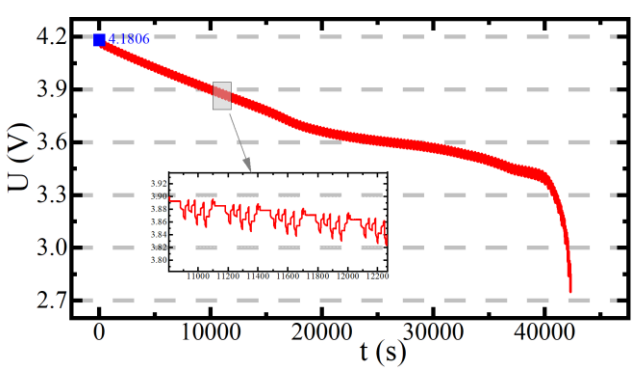

(a) Voltage curve of the BBDST condition

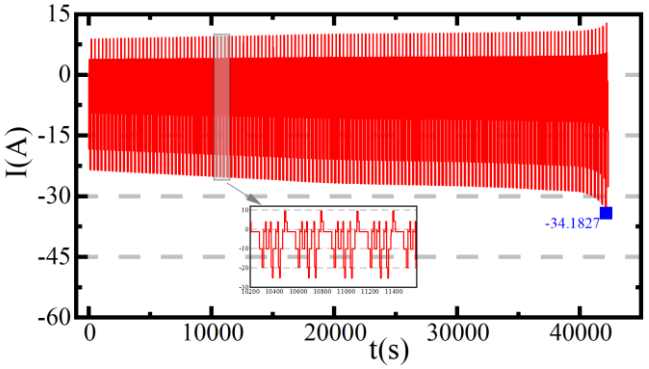

(b) Current curve of the BBDST condition

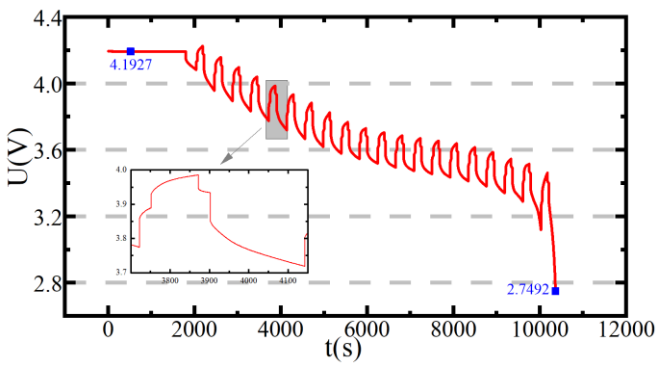

(c) Voltage curve of the DST condition

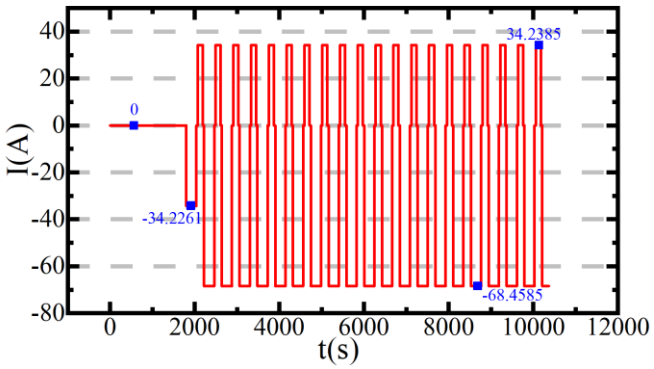

(d) Current curve of the DST condition

Figure 7. The charts of experimental data under BBDST and DST conditions

In Figure 7, (a) and (b) are the experimental current and voltage curves of the BBDST working condition, respectively. Since the BBDST condition is to discharge the battery, it can be found that as the number of cycles increases, the current shows an increasing trend and the terminal voltage shows a decreasing trend.

After the parameters are identified online by the RLS method, a Thevenin equivalent circuit model is established. In order to verify the validity of the model, the simulated terminal voltage and the experimental terminal voltage under BBDST and DST conditions are compared, respectively. And the current value measured at this time is used as the input value. The simulated and experimental terminal voltages are shown in Figure 8.

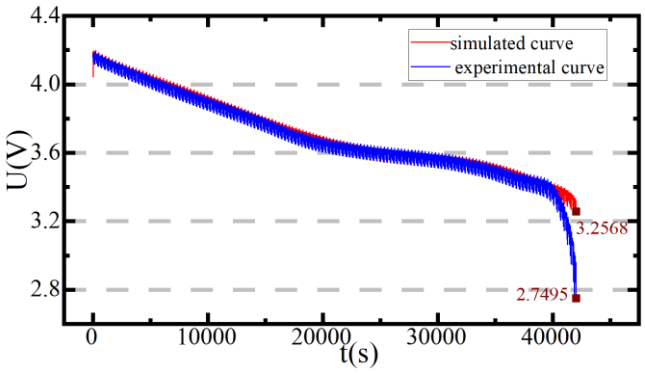

(a) The voltage curves under the BBDST condition

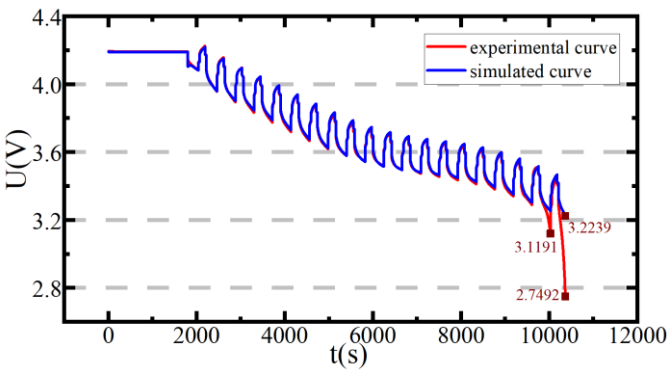

(b)The voltage curves under the DST condition

Figure 8. The charts of simulated and experimental terminal voltages

It can be seen from Figure 8that the simulated curves and the experimental curves have the same trend, which verifies that the algorithm can effectively simulate the battery discharge under BBDST and DST conditions. Based on the ST-DAEKF algorithm, the SOC of the lithium-ion battery under BBDST

and DST conditions is estimated. The initial value of the given SOC is 0.95 to compare the convergence between the various algorithms. The experimental results of SOC are shown in Figure 9.

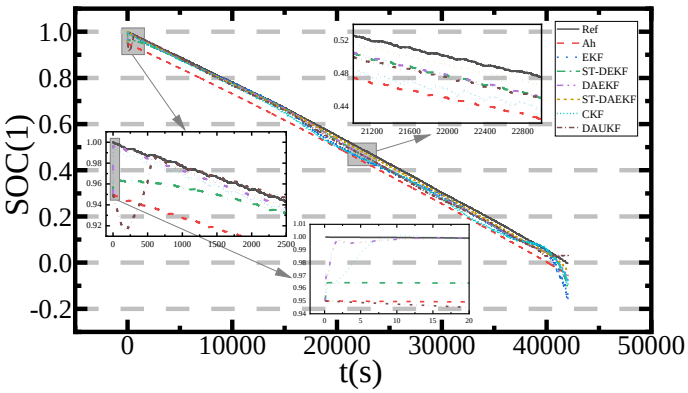

(a) SOC results of various algorithms under the BBDST condition

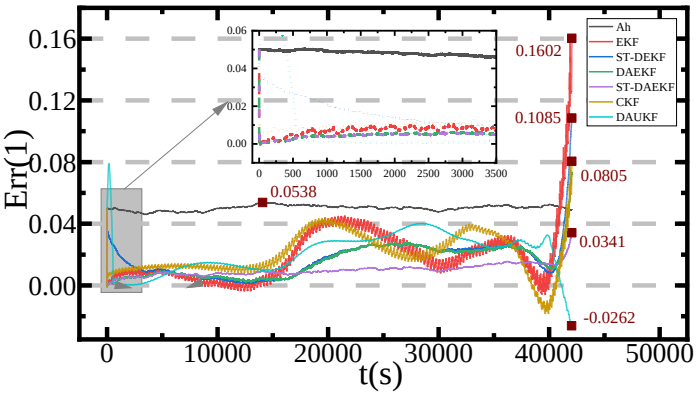

(b) SOC errors of various algorithms under the BBDST condition

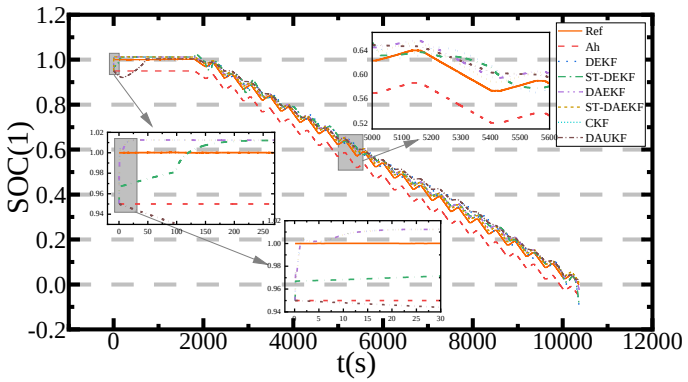

(c) SOC results of various algorithms under the DST condition

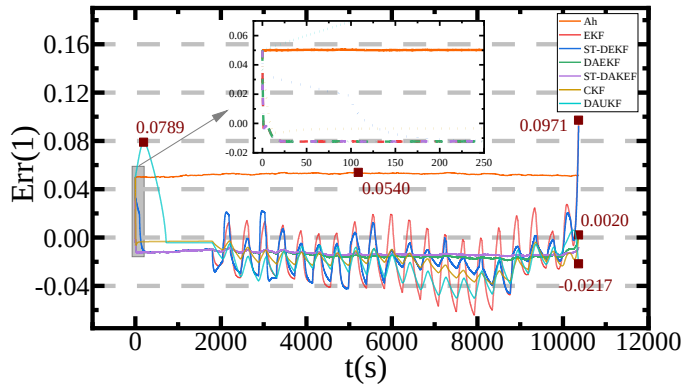

(d) SOC errors of various algorithms under the DST condition

Figure 9. The charts of SOC results and errors under different conditions

Figure 9(a) and (b) are charts of SOC estimation results of different algorithms under BBDST and DST conditions, respectively. The algorithms include the ampere-hour integration method, the EKF algorithm, the dual adaptive extended Kalman algorithm (DAEKF)[50], the strong tracking-dual extended Kalman filter (ST-DEKF)[48], the strong tracking-dual adaptive extended Kalman filter (ST-DAEKF) algorithm, the cubature Kalman filter (CKF) algorithm[24, 51] and the dual adaptive unscented Kalman filter (DAUKF) algorithm[35, 52]. *Ref* represents the reference value of the SOC. Figure 9(b) and (d) are the error curves obtained by subtracting the SOC value of different algorithms from the SOC reference value under these two conditions, respectively. It can be seen from Figure 9 that the average estimation error of SOC based on the Thevenin model and ST-DAEKF algorithm is 0.99%, the maximum estimation error after convergence is 3.41%, and the convergence time is 15 seconds under the BBDST condition. And under the DST condition, the corresponding data is 1.29%, 1.56%, and 20 seconds, respectively. Compared with other algorithms, the ST-DAEKF algorithm can correct the error of the initial value of SOC better and faster, and the estimation accuracy of SOC is also higher. Besides,

under these two conditions, the converge speed of ST-DAEKF algorithm is significantly faster than that of DAUKF algorithm which described in document [52]. Although the mean estimation error of CKF algorithm which used in literature [51] is small with the value of 1.62% and 1.87% under the BBDST condition and the DST condition, the error of the proposed ST-DAEKF algorithm is smaller than that of CKF algorithm. Based on the ST-DAEKF algorithm and its corresponding estimation results of SOC value, the SOH of the lithium-ion battery under BBDST and DST conditions is estimated. The reference value of capacity is 69.0083Ah and the experimental results of SOH are shown in Figure 10.

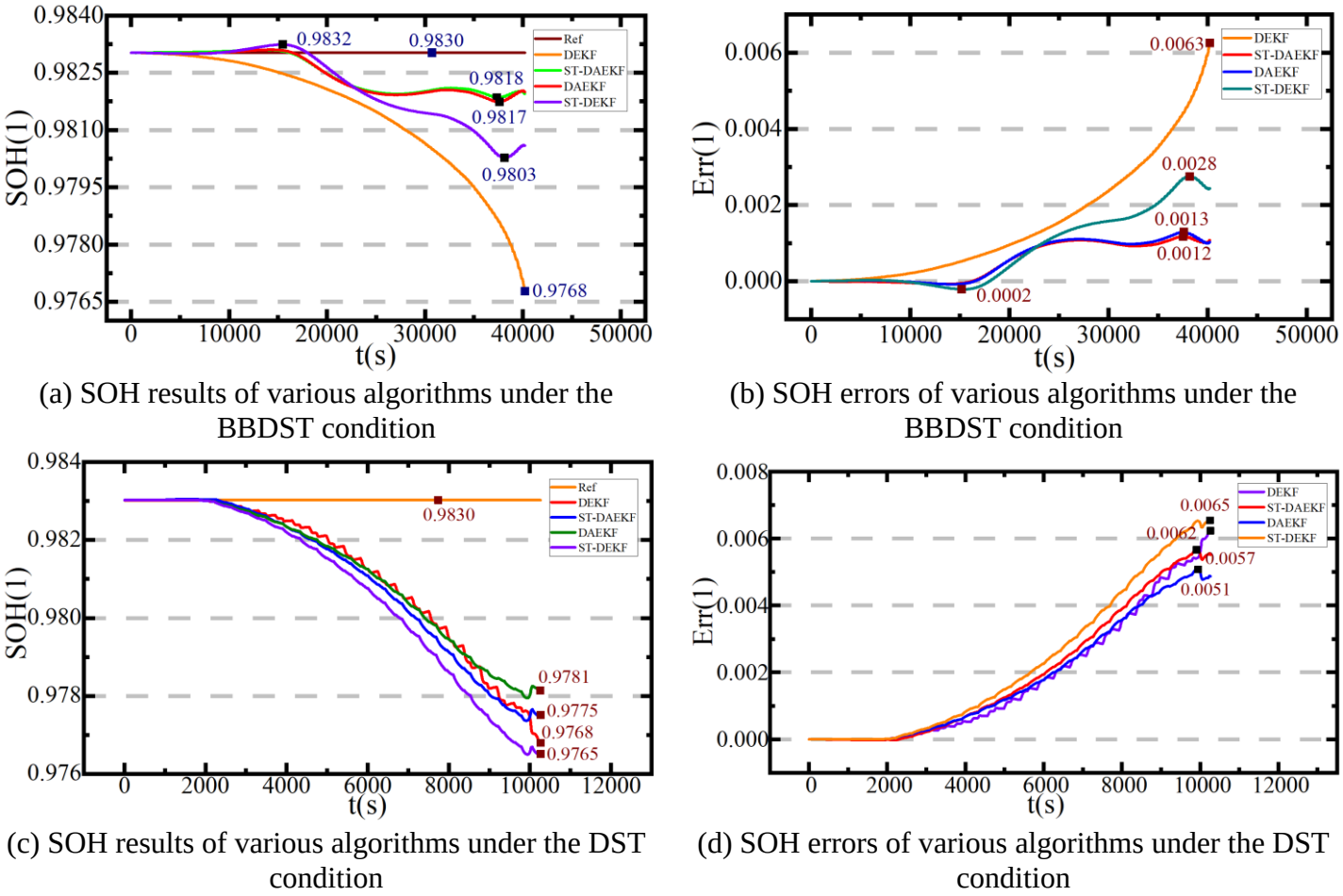

(a) SOH results of various algorithms under the BBDST condition

(b) SOH errors of various algorithms under the BBDST condition

(c) SOH results of various algorithms under the DST condition

(d) SOH errors of various algorithms under the DST condition

Figure 10. The charts of SOH results and errors under different conditions

Figure 10(a) and (b) are charts of SOH estimation results of different algorithms under BBDST and DST conditions, respectively. Figure 10(b) and (d) are the error curves obtained by subtracting the SOH value of different algorithms from the SOC reference value under these two conditions, respectively. It can be seen from Figure 10 that under the BBDST condition, the average estimation error of SOH based on the Thevenin model and ST-DAEKF algorithm is 0.06%, the maximum estimation error is 0.12%. And under the DST condition, the corresponding data is 0.23% and 0.66%, respectively, which is much smaller than the errors of other algorithms, especially the EKF algorithm. In addition, it

can be found from Figure 10(a) and (c) that the estimated SOH value shows a slowly decreasing trend, which is in line with the actual situation that the rated capacity of the battery decreases with use. The above results verify the improvement effect of the ST-DAEKF algorithm.

4. CONCLUSIONS

In order to realize the real-time estimation of the SOC and SOH of the lithium-ion battery of electric vehicles, considering the tracking ability of the system and the ability to estimate and modify the statistical characteristics of noise, this paper proposes a novel joint estimation method of SOC and SOH based on the strong tracking-dual adaptive extended Kalman filter (ST-DAEKF) algorithm to establish a joint estimation model. The BBDST condition and DST conditions at 25 ℃ are used for online parameter identification, model verification, and battery state estimation. The results of the algorithm simulation show that under the BBDST condition, the maximum SOC error and the average error are 3.41% and 0.99%, respectively, with the corresponding convergence time of 15 seconds. And under the DST condition, the corresponding data is 1.56%, 1.29%, and 20 seconds, respectively. Meanwhile, under the BBDST condition, the maximum SOH error and average error are 0.12% and 0.06%, with the corresponding data of 0.66% and 0.23% under the DST condition. The estimated SOC and SOH errors under the above two working conditions are relatively small, which verifies the reliability of the algorithm and achieves the expected design effects. The accurate SOC and SOH estimation for electric vehicles promotes the development of related battery management systems, improves the working efficiency of electric vehicles and the use efficiency of their lithium-ion batteries, and avoids a series of problems caused by excessive errors in battery SOC and SOH estimation.

ACKNOWLEDGMENTS
The work was supported by National Natural Science Foundation of China (No. 61801407).

References

1. X. Li, Z. Huang, J. Tian and Y. Tian, *Energy*, 220 (2021) 119767.
2. G. Javid, O.A. Djaffar and B. Michel, *Energies*, 14 (2021) 758.
3. H. Farzin, M. Fotuhi-Firuzabad and M. Moeini-Aghtaie, *IEEE Trans. Sustainable Energy*, 7 (2017) 1730.
4. Z. Chen, L. Yang, X. Zhao, Y. Wang and Z. He, *Appl. Mathe. Modelling*, 70 (2019) 532.
5. X. Zhu, FM. Lucia, J. Joris, DH. Joris, N. Alexandros, O. Noshin and H. Annick, *Electrochim. Acta*, 287 (2018) 10.
6. N.P.A. Muhammad, D.S. Artono, and W. Hendri, *J. Phys. Conf. Series*, 1 (2021) 1825.
7. Y. Luo, P. Qi, Y. Kan, J. Huang, H. Huang, J. Luo, J. Wang, Y. Wei, R. Xiao and S. Zhao, *Int. J. Energ. Res.*, 44 (2020) 10538.
8. K. Liu, X. Hu, Z. Yang, Y. Xie and S. Feng, *Energ. Convers. Manage.*, 195 (2019) 167.
9. X. Hu, K. Zhang, K. Liu, X. Lin, S. Dey and S. Onori, *IEEE Ind. Electron. Magazine*, 14 (2020) 65.
10. F. Feng, X. Hu, L. Hu, F. Hu, Y. Li and L. Zhang, *Renew. Sustain. Energ. Rev.*, 112 (2019) 102.
11. Y. Fan, Y. Bao, C. Lin, Y. Chu, X. Tan and S. Yang, *Appl. Ther. Eng.*, 155 (2019) 96.
12. X. Rui, L. Li and J. Tian, *J. Power Sources*, 405 (2018) 18.
13. X. Tan, D. Zhan, P. Lyu, J. Rao and Y. Fan, *J. Power Sources*, 484 (2021) 229233.

14. R. Zhang, B. Xia, B. Li, L. Cao, Y. Lai, W. Zheng, H. Wang and W. Wang, *Energies*, 11 (2018) 1820.
15. C.R Lashway and O.A. Mohammed, *IEEE Trans. Transport. Electrific.*, 2 (2016) 454.
16. AB. Ahmad, CA. Ooi, D. Ishak and J. Teh, *Qualit. Cont. Trans.*, 7 (2019) 131.
17. U. Westerhoff, T. Kroker, K. Kurbach, M.Kurrat, *J. Energy Storage*, 8 (2016) 244.
18. J. Zhang, P. Wang, Y. Liu and Z. Cheng, *Energies*, 14(2021) 769.
19. D.I. Stroe, M. Swierczynski, A.I. Store, S. K. Kaer and R. Teodorescu, *IET Renew. Power Gener.*, 11 (2017) 1136.
20. H. Sheng and J. Xiao, *J. Power Sources.* 281 (2015) 131.
21. D. Jiménez-Bermejo, J. Fraile-Ardanuy, S. Castaño-Solis, J. Merino and R. Álvaro-Hermana, *Proced. Comp. Sci.*, 130 (2018) 533.
22. B. Xia, D. Cui, S. Zhen, Z. Lao, R. Zhang, W. Wei, S. Wei, Y. Lai and M. Wang, *Energy*, 153 (2018) 694.
23. M. Jiao, D. Wang and J. Qiu, *J. Power Sources*, 459 (2020) 228051.
24. Y. Tian, R. Lai, X. Li, L. Xiang and J. Tian, *Appl. Energy*, 265 (2020) 114789.
25. E. Chemali, P. J. Kollmeyer, M. Preindl and A. Emadi, *J. Power Sources*, 400 (2018) 242.
26. C. Li, F. Xiao and Y. Fan, *Energies*, 12 (2019) 1592.
27. C. Ruhatiya R. Gandra, P. Kondaiah, K. Manivas, A. Samhith, L. Gao, J. S. Lam and A. Garg, *Int. J. Energ. Res.*, 45 (2020) 6152.
28. B. Xiao, B. Xiao and L. Liu, *Int. J. Energ. Res.*, 45 (2021) 5695.
29. B. Wei, D. Legut, S. Sun, H. Wang and R. Zhang, *Mater. & Des.*, 202 (2021) 109555.
30. Q. Wang, J. Wang, P. Zhao, J. Kang, F. Yan and C. Du, *Electrochim. Acta*, 228 (2017) 146.
31. G. Chen, Y. Liu, S. Wang, Y. Luo and Z. Yang, *J. Energy Storage*, 33 (2021) 101933.
32. J.H. Kwon, S. Jo, K.Y. Cho and K.S. Eom, *J. Power Sources*, 473 (2020) 228587.
33. L. Li, M. Hu, Y. Xu, C. Fu and Z. Li, *Appl. Sci.*, 10 (2020) 6371.
34. B. Ren, C. Xie, X. Sun, Q. Zhang and D. Yan, *IET Power Electron.*, 13 (2020) 2531.
35. S. Zhang, X. Guo and X. Zhang, *J. Energy Storage*, 32 (2020) 101980.
36. K. Zhang, P. Zhao, C. Sun, Y. Wang and Z. Chen, *Chinese J. Aeronautics.* 33 (2020) 1517.
37. K. Yang, Y. Tang and Z. Zhang, *Energies*, 14 (2021) 1054.
38. S. Khaleghi, Y. Firouz, J.V. Mierlo and P.V.D. Bossche, *Appl. Energy*, 255 (2019) 113813.
39. M. Lucu, E. Martinez-Laserna, I. Gandiaga and H. Camblong, *J. Power Sources*, 401 (2018) 85.
40. S. Huang, T. Kuo-Hsin, J. Liang, C. Chang and P. Michael, *Energies*, 10 (2017) 512.
41. N. Wassiliadis, J. Adermann, A. Frericks, M. Pak, C. Reiter, B. Lohmann and M. Lienkamp, *J. Energy Storage*, 19 (2018) 73.
42. M. Zeng, P. Zhang, Y. Yang, C. Xie and Y. Shi, *Energies*, 12 (2019) 3122.
43. J. Park, M. Lee, G. Kim, S. Park and J. Kim, *Energies*, 13 (2020) 2138.
44. M. Gholizadeh and A. Yazdizadeh, *IET Electric. Sys. Transport.*, 10 (2020) 135.
45. B. Ren, C. Xie, X. Sun, Q. Zhang and D. Yan, *IET Power Electron.*, 13 (2020) 2531.
46. R. Havangi, *Electric. Eng.*, 1 (2021) 1.
47. J. Xu, W. Xu, F. Huang, W. Xia and B. Liu, *IOP Conf. Series: Earth and Envir. Sci.*, 721 (2021) 12002.
48. J. Wei, G. Dong and Z. Chen, *Energ. Pro.*, 158 (2019) 2500.
49. X. Chen, X. Chen and X. Chen, *Int. J. Energ. Res.*, 45 (2021) 13238.
50. W. Xu, S. Wang, C. Jiang, F. Carlos, C. Yu, Y. Fan, W. Cao, *Int. J. Energ. Res.*, 45 (2021) 14592.
51. J. Peng, J. Luo, H. He and B. Lu, *Appl. Energ.*, 253 (2019) 1.
52. F. Sun, X. Hu, Y. Zou and S. Li, *Energy*, 36 (2011) 3531.